Supplemental information

Peroxisomal L-bifunctional protein (EHHADH) deficiency causes male-specific kidney hypertrophy and proximal tubular injury in mice

Pablo Ranea-Robles, Kensey Portman, Aaron Bender, Kyung Lee, John Cijiang He, David J. Mulholland, Carmen Argmann, Sander M. Houten

Table of Contents

Supplementary Figure S1. **EHHADH deficiency does not cause morphological or functional changes in female mouse kidneys.**

A) Representative images of H&E and PAS staining in kidney sections from female WT and *Ehhadh* KO mice. Scale bars = 100 µm. **B**) Morphometric analysis of the cross-sectional tubule areas in WT (n=2) and *Ehhadh* KO (n=3) female mice. **C**) Glomerular filtration rate (GFR) in WT and *Ehhadh* KO female mice (n=3 per genotype). **D**) Blood urea nitrogen (BUN) levels (mg/dL) in WT (n=3) and *Ehhadh* KO (n=4) female mice. Data are presented as mean ± SD with individual values plotted.

Supplementary Figure S2. **Transcriptomics of male *Ehhadh* KO kidneys**

Pathway enrichment analysis of genes either significantly up- or down- regulated in *Ehhadh* KO mice versus WT according to Hallmark (**A**) or BioPlanet (**B**) databases. Values represent the fold enrichment and significance is indicated as * adj p<0.05. All BioPlanet pathways shown are significantly enriched as adj p <0.05 and only pathways with fold enrichment >3.0 are shown. Full table of results are in Table S1B and S1C.

Supplementary Figure S3. EHHADH deficiency activates the proximal tubule injury response in male mice.

A) Immunoblots of KIM-1 and SOX-9, and their loading control α-Tub (alpha-tubulin). SOX-9 protein levels were quantified relative to α-Tub. Several bands showed in the KIM-1 blot correspond to non-specific bands (#), as reported elsewhere [1]. This is in line with the absence of KIM-1 signal in IF studies in WT kidneys. The quantified band for SOX-9 is marked with a black arrowhead. **B)** Representative image of SGLT1 (red) and EHHADH (green) co-immunostaining in the cortical area of a WT mouse kidney. **C**) Representative image of SLC34A3 (red) and EHHADH (green) co-immunostaining in the cortical area of a WT mouse kidney. Two S1 segments are marked. **D**) Representative image of SGLT1 (green) and KIM-1 (red) co-immunostaining in the cortical area of an *Ehhadh* KO male kidney. **E**) Representative image of SLC34A3 (green) and KIM-1 (red) co-immunostaining in the cortical area of an *Ehhadh* KO male kidney. **F**) Representative image of CALB (green) and KIM-1 (red) co-immunostaining in an *Ehhadh* KO male kidney. **G**) Representative image of AQP2 (green) and KIM-1 (red) co-immunostaining in an *Ehhadh* KO male kidney. Data are presented as mean ± SD with individual values plotted. Statistical significance was tested using unpaired t test with Welch's after multiple comparison correction *P < 0.05. Scale bar = 100 µm.

Supplementary Figure S4. Pathway enrichment analysis of sexually dimorphic DEGs in mouse kidneys

A) Top 5 significant MSigDB Hallmarks terms and GO Cellular Component terms after pathway enrichment analysis using DEGs from Si et al [2]. B) Top 5 significant MSigDB Hallmarks terms and GO Cellular Component terms after pathway enrichment analysis using DEGs from Wu et al [3]. Terms were ranked by -log10(adj p).

Supplementary Figure S5. The kidney phenotype caused by EHHADH deficiency in mice is androgen-dependent

A) Kidney-to-BW ratio progression with age in male WT and *Ehhadh* KO mice. **B**) Kidney-to-BW ratio in sham-operated (n=2 per genotype) and orchiectomized (n=3 per genotype) WT and *Ehhadh* KO male mice. Statistical significance was tested using two-way ANOVA with "Genotype" and "Orchiectomy" as the two factors. *P < 0.05; ***P < 0.001. Scale bars = 100 µm

Supplementary Figure S6. **Proposed working models to explain how EHHADH deficiency causes male-specific PT injury**

References

1. Ichimura T, Hung CC, Yang SA, Stevens JL, Bonventre J V.: Kidney injury molecule-1: A tissue and urinary biomarker for nephrotoxicant-induced renal injury. *Am. J. Physiol. - Ren. Physiol.* 286: 2004

2. Si H, Banga RS, Kapitsinou P, Ramaiah M, Lawrence J, Kambhampati G, Gruenwald A, Bottinger E, Glicklich D, Tellis V, Greenstein S, Thomas DB, Pullman J, Fazzari M, Susztak K: Human and murine kidneys show gender- And species-specific gene expression differences in response to injury. *PLoS One* 4: e4802, 2009

3. Wu H, Lai CF, Chang-Panesso M, Humphreys BD: Proximal tubule translational profiling during kidney fibrosis reveals proinflammatory and long noncoding RNA expression patterns with sexual dimorphism. *J. Am. Soc. Nephrol.* 31: 23–38, 2020

Supplementary Figure S1

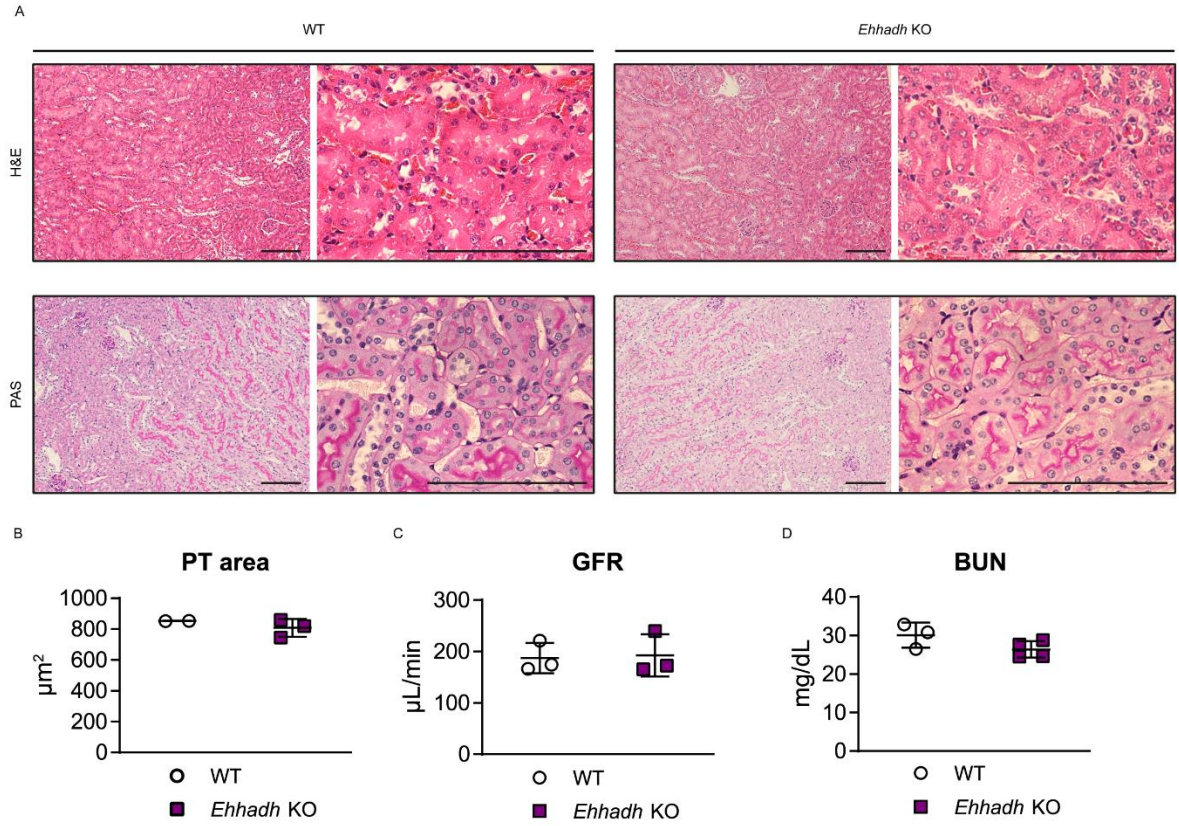

Supplementary Figure S2

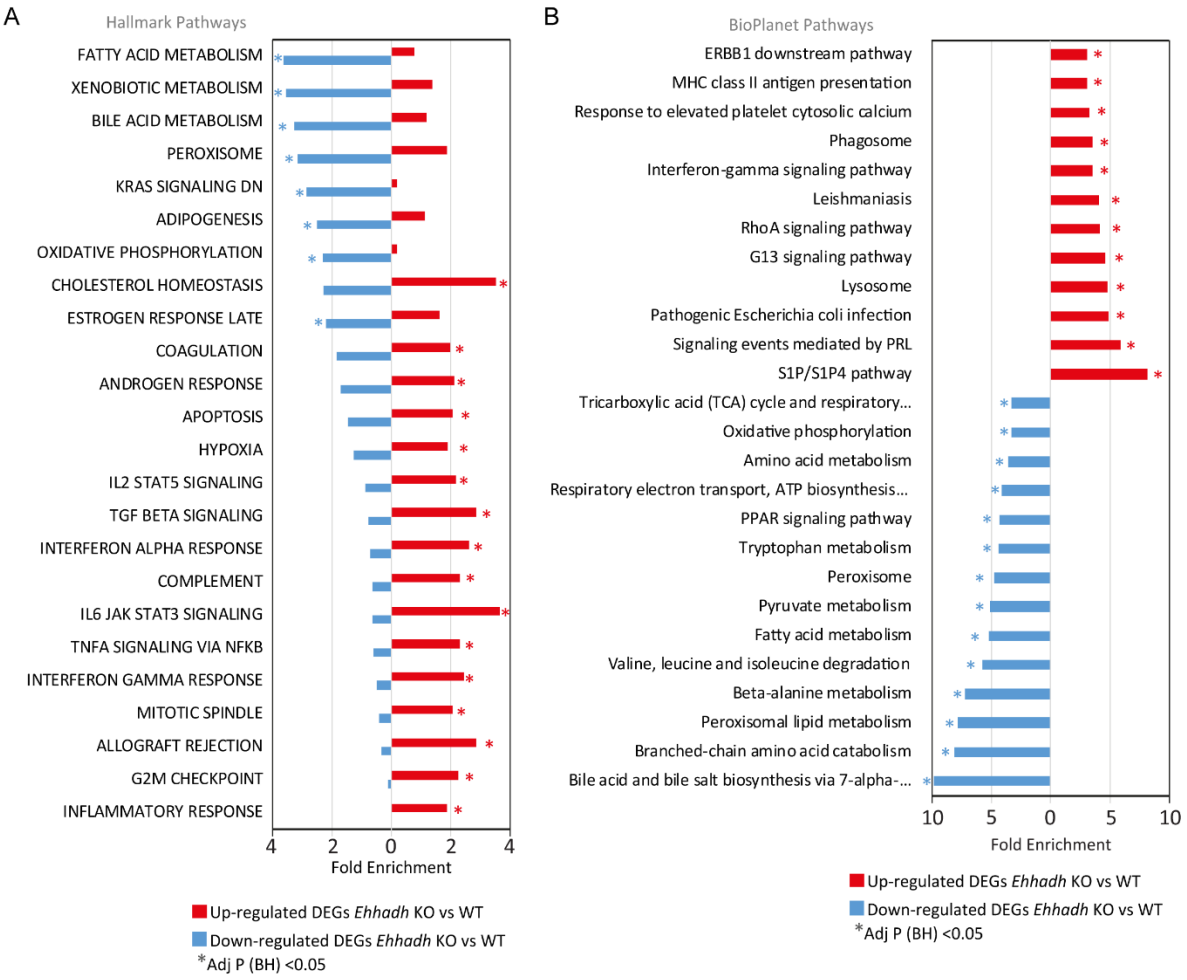

Supplementary Figure S3

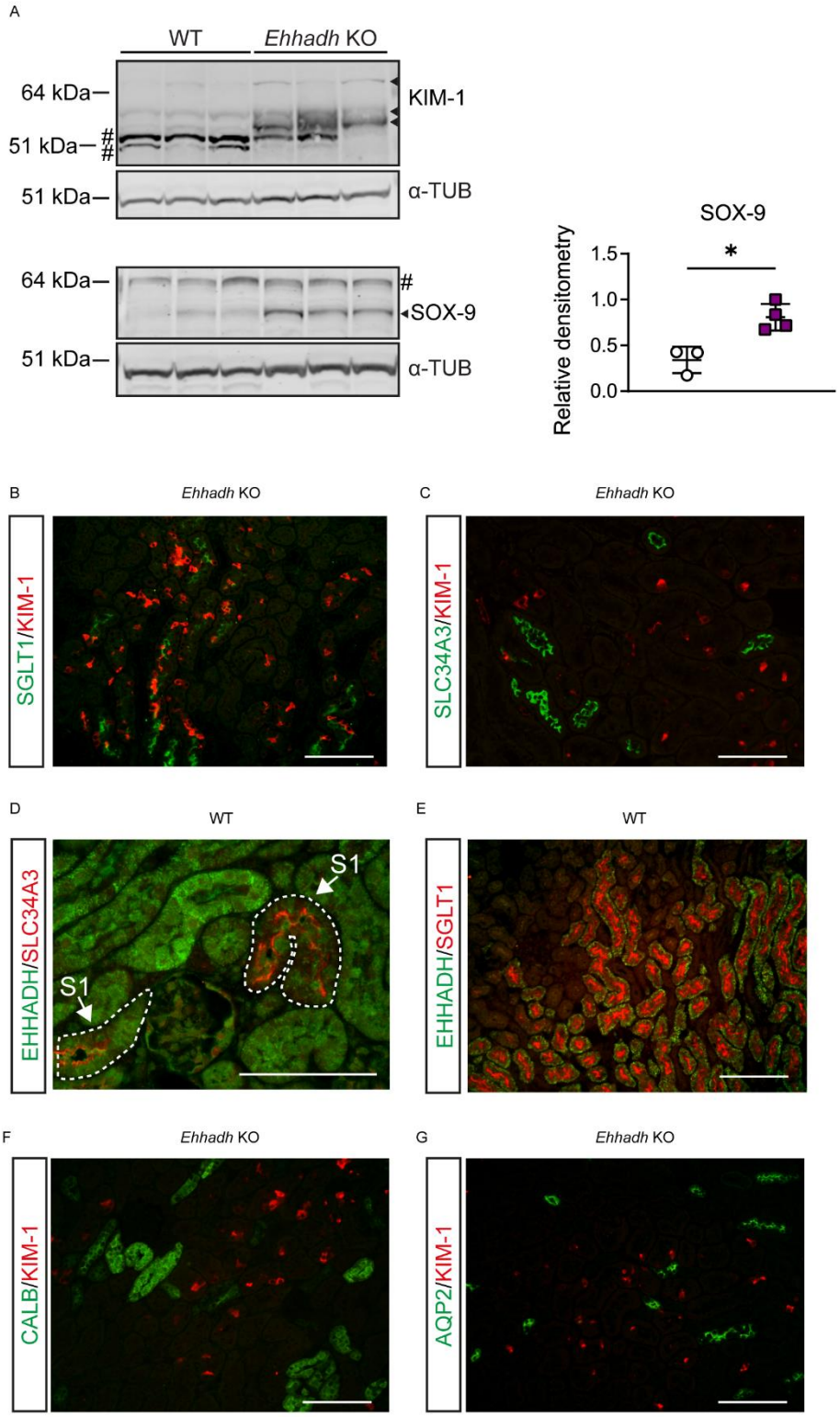

Supplementary Figure S4

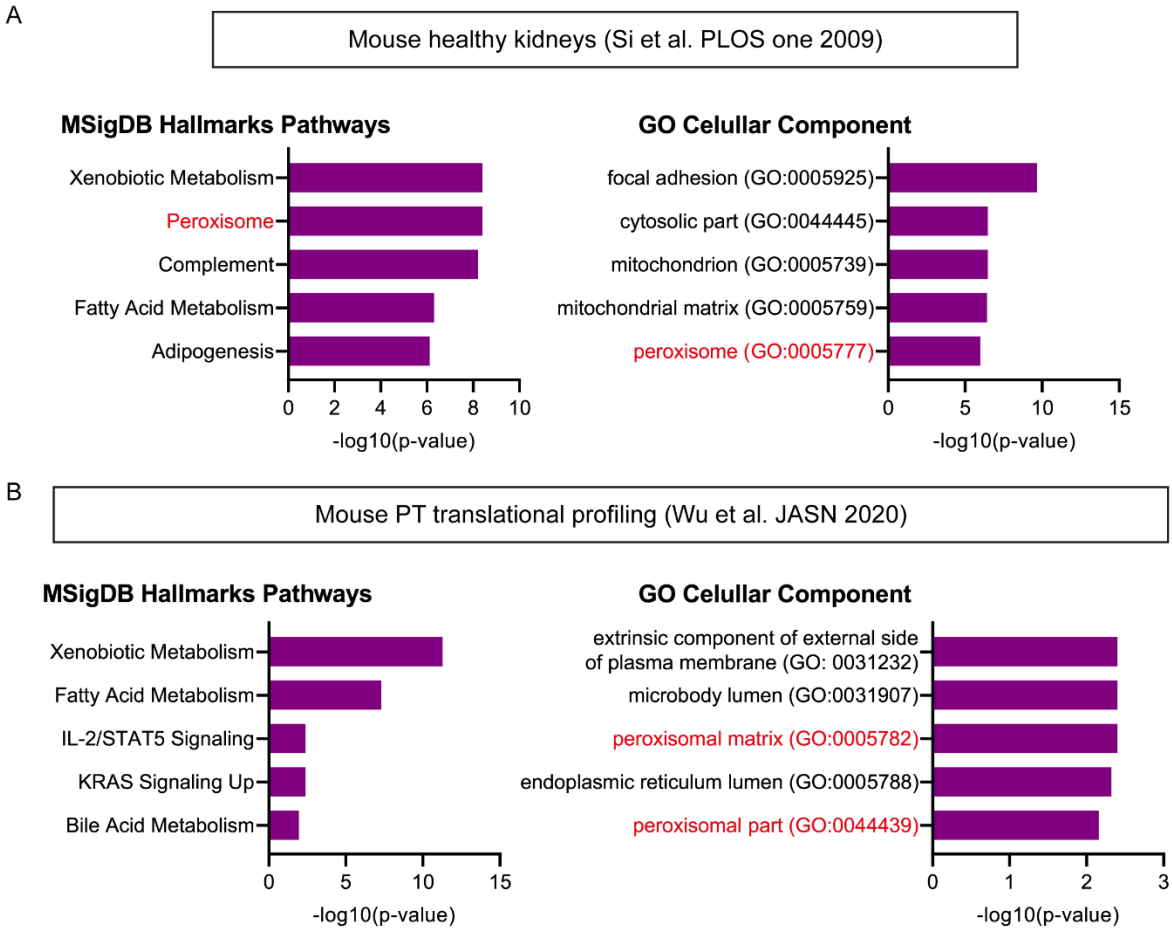

Supplementary Figure S5

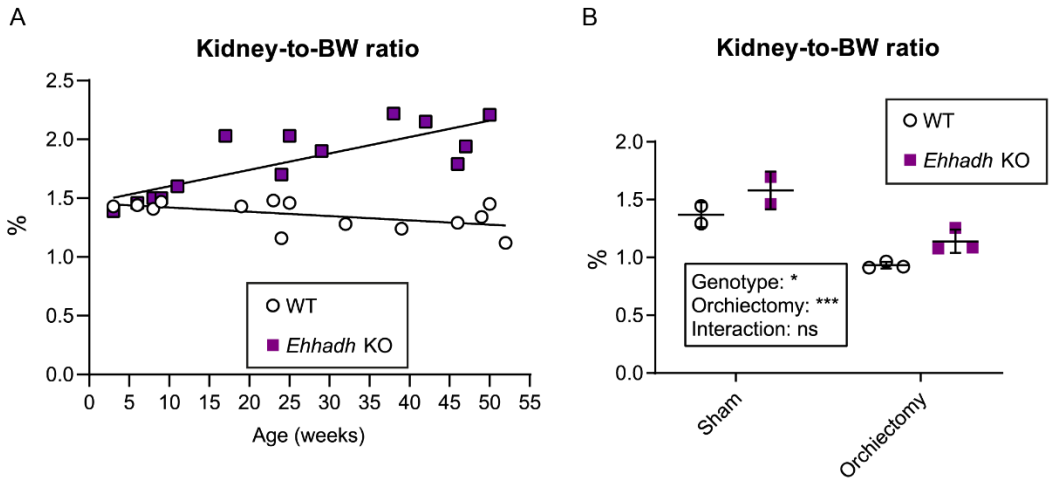

Supplementary Figure S6